J. Phase Equilib. Diffus. (2022) 43:214–228
https://doi.org/10.1007/s11669-022-00953-w

Thermodynamic Modeling of the Co-Cu-Sn Ternary System

Dongyu Cui[1] · Jiong Wang[1] · Na Yan[2]

Submitted: 24 November 2021 / in revised form: 24 February 2022 / Accepted: 22 March 2022 / Published online: 3 May 2022

Abstract The Co-Cu-Sn ternary system has been modeled based on reported phase equilibrium data in the literature using the CALPHAD (CALculation of PHAse Diagrams) method. The excess Gibbs energies of solution phases, including liquid, Bcc, Fcc and Hcp, are expressed by the Redlich-Kister polynomial. The two-sublattice model $(Co,Cu)_m(Sn)_n$ is used to describe the solid solution of binary intermetallic compounds, i.e. $CoSn_3$, $CoSn_2$ Cu_3Sn and βCu_6Sn_5 in the Co-Cu-Sn ternary system. Co_3Sn_2 was described using the four-sublattice model $(Co,Cu,Sn)_1(Cu,Sn)_1(Co,Va)_{0.5}(Co,Va)_{0.5}$. The ternary stoichiometric compound $Co_2Cu_8Sn_3$ is modeled by the stoichiometric model, $Co_2Cu_{7.5}Sn_3$. Finally, a set of self-consistent parameters which can describe the thermodynamics of the Co-Cu-Sn ternary system was obtained. Based on the calculated thermodynamic parameters, the liquidus projection and reaction scheme are also derived in the present work.

Keywords CALPHAD · Co-Cu-Sn system · gibbs energy · phase equilibria · thermodynamic

✉ Jiong Wang
wangjionga@csu.edu.cn

[1] Powder Metallurgy Research Institute, Central South University, Changsha 410083, Hunan, China

[2] School of Physical Science and Technology, Northwestern Polytechnical University, Xian 710072, China

1 Introduction

The welding technique is widely used in aerospace, automotive, electronics and etc.[1–5] Meanwhile, it is inevitable that lead-free solder is becoming a substitute for tin-lead solder with increasing environmental protection requirements. Among various kinds of lead-free solders, Ag-Sn-Cu, Ag-Sn and Cu-Sn alloys are the most dominant due to their high-temperature performance.[6–8] Since Ag is an expensive material which could increase the cost of production, Co-doped Cu-Sn alloys are becoming the promising candidates for lead-free solders,[9–11] which have good performance and low cost. In addition, the Co-Cu binary system exhibits metastable liquid-liquid separation,[12,13] which can be influenced by doping elements. Curiotto et al.[14] investigated the mechanism of liquid demixing and formation of microstructures in the Co-Cu binary system with the addition of Ni. Liquid demixing was found to be restrained with increasing Ni content. However, the effect of Sn on the liquid demixing of the Co-Cu-Sn system is still unknown.

In order to understand the Co-Cu-Sn ternary system well and guide the material design of the lead-free solder, an accurate thermodynamic description of the Co-Cu-Sn ternary system is required.[15] In previous studies, Chen et al.[16] measured the isothermal sections of the Co-Cu-Sn ternary system. Liu et al.[17] measured the temperatures of transformation in the $Co_{0.5}Cu_{0.5}$-Sn section. However, the accurate thermodynamic description of the Co-Cu-Sn ternary system has not been reported.

For these reasons, the aim of the present work is to obtain a self-consistent thermodynamic description for the Co-Cu-Sn ternary system combined with the experimental phase equilibrium data and the evaluated Co-Cu, Co-Sn and Cu-Sn systems in the literature. The effect of Sn

addition on the liquid-liquid phase separation also needs to be studied.

2 Review of Literature

The research results for the Co-Cu-Sn ternary system and its boundary binary systems are reviewed. The Co-Cu, Co-Sn and Cu-Sn binary phase diagrams are calculated using the selected thermodynamic parameters[18–22] and shown in Fig. 1(a)-(c) respectively. In addition, the crystal information of the phases in the Co-Cu-Sn ternary system is summarized in Table 1 according to the literature.[16,23–34]

2.1 The Co-Cu Binary System

The Co-Cu system has been assessed by many researchers.[18,35–40] Kaufman[35] and Hasebe and Nishizawa[36] assessed the Co-Cu binary system early. However, the SGTE (Scientific Group Thermodata

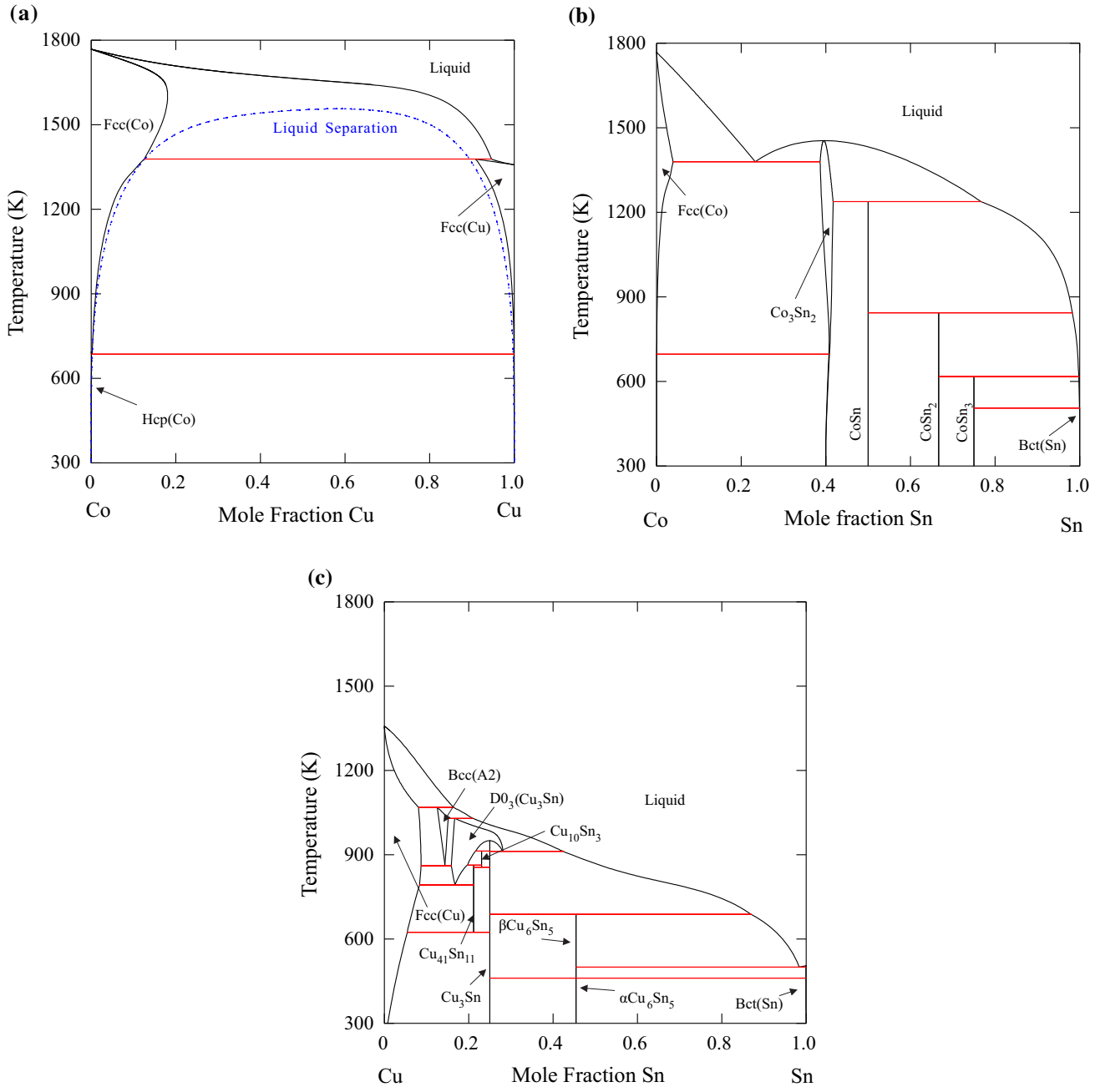

Fig. 1 The boundary binary systems selected in this work (a) Co-Cu[18]; (b) Co-Sn[19]; (c) Cu-Sn[21]

Table 1 Crystal structures of solid phases in the Co-Cu-Sn ternary system

Phase	Space group	Prototype	Pearson symbol	Lattice parameter, nm			Ref.
				a	*b*	*c*	
Fcc(Co)	$Fm\ \bar{3}\ m$	Cu	*cF*4	0.3554			Ref 23
Hcp(Co)	$P6_3/mmc$	Mg	*hP*2	0.2507		0.4068	Ref 24
Fcc(Cu)	$Fm\ \bar{3}\ m$	Cu	*cF*4	0.3615			Ref 24
Bct(Sn)	$I4_1/amd$	βSn	*tI*4	0.5832		0.3182	Ref 24
αCo_3Sn_2	*Pnma*	Ni_3Sn_2	*oP*20	0.7085	0.5216	0.8194	Ref 25
βCo_3Sn_2	$P6_3/mmc$	Ni_2In	*hP*6	0.4162		0.5233	Ref 25
CoSn	*P6/mmm*	CoSn	*hP*6	0.5279		0.4259	Ref 26
$CoSn_2$	*I4/mcm*	$CuAl_2$	*tI*12	0.6363		0.5458	Ref 27
$\alpha CoSn_3$	*Cmca*	$PbSn_3$	*oC*32	1.6864	0.6268	0.6270	Ref 28
$\beta CoSn_3$	$I4_1/acd$	$\beta CoSn_3$	*tI*64	0.6275		3.3740	Ref 28
$Cu_{10}Sn_3$	$P6_3$	AgZn	*hP*26	0.7330		0.7864	Ref 29
$Cu_{41}Sn_{11}$	$F\ \bar{4}\ 3m$	$Cu_{41}Sn_{11}$	*cF*416	1.7980			Ref 30
Bcc(A2)	$Im\ \bar{3}\ m$	W	*cI*2	0.3030			Ref 31
$D0_3(Cu_3Sn)$	$Fm\ \bar{3}\ m$	BiF_3	*cF*16	0.3039-0.3057			Ref 31
Cu_3Sn	*Cmcm*	Cu_3Ti	*oC*80	0.5529	4.7750	0.4323	Ref 32
αCu_6Sn_5	*C2/c*	Cu_6Sn_5	*mC*44	1.1036	0.7288	0.9841	Ref 33
βCu_6Sn_5	$P6_3/mmc$	NiAs	*hP*4	0.4192		0.5037	Ref 34
$Co_2Cu_8Sn_3$	…	…	…	1.79			Ref 16

Europe)[41] database for pure elements is not used in their work, which may cause incompatibility when extrapolating to high-order systems. Then, Kubista and Vrestal[37] measured the molar excess Gibbs energy, enthalpy, entropy of mixing and activities in the liquid phase. In addition, Kubista and Vrestal[37] reassessed the Co-Cu binary system by describing the liquid phase by TAP (Thermodynamically Adapted Power) and Redlich-Kister polynomials[42] respectively. However, the parameters cannot describe the phase diagram well if the Hcp and Bcc phases are not suspended. Therefore, Yu et al.[40] adjusted the thermodynamic parameters by adding positive interaction parameters for the Hcp and Bcc phases, but the error for the solidus still existed. Considering the metastable miscibility gap, Palumbo et al.[18] and Turchanin and Agraval[38] reoptimized the Co-Cu system. The results provided by Palumbo et al.[18] agree well with the experimental activity and mixing enthalpy data. Later, the parameters of binary interaction for the Bcc phase provided by Turchanin and Agraval[38] were modified by Turchanin et al.[39] Considering the more accurate activity, the parameters determined by Palumbo et al.[18] are adopted in the present work.

2.2 The Co-Sn Binary System

The Co-Sn binary system has been assessed by Liu et al.,[43] Jiang et al.,[20] Vassilev and Lilova,[44] Dong et al.[19] and Jedlickova. et al.[45] respectively. However, the results determined by Liu et al.[43] present an upturned miscibility gap of the liquid phase above 2000K. In addition, the liquidus calculated by Vassilev and Lilova[44] shows a margin of error of approximately 5% on the Sn-rich side. Jiang et al.[20] assessed the Co-Sn binary system showing good agreement with the experimental activity data. Dong et al.[19] modified the parameters of $CoSn_2$ and $CoSn_3$ reported by Jiang et al.[20] The revised parameters are successfully used to reproduce the Ag-Co-Sn ternary system. For these reasons, the parameters provided by Jiang et al.[20] and Dong et al.[19] are adopted to build the Co-Cu-Sn ternary database.

2.3 The Cu-Sn Binary System

The Cu-Sn binary system has been evaluated and modified by many researchers.[21,22,46–53] The thermodynamic description was carried out by Shim et al.[21] and slightly modified by Moon et al.[46] Miettinen[47] optimized the Cu-rich side of the Cu-Sn binary system, but there exists a stable $D0_3(Cu_3Sn)$ phase above 3000K. For this reason, Li et al.[51] reassessed the Cu-Sn binary system. However, liquid-liquid phase separation was observed above 5500K. Considering the solubility of Cu_3Sn and Cu_6Sn_5, Gierlotka et al.[49] reassessed this system. Liu et al.[48] modeled the Bcc phase by a two sublattice model, $(Cu,Sn)_{0.5}(Cu,Sn)_{0.5}$, to describe the order-disorder transformation of the Bcc phase. Li et al.[52] reassessed the system using a four sublattice model $(Cu,Sn)_{0.25}(Cu,Sn)_{0.25}(Cu,Sn)_{0.25}(Cu,Sn)_{0.25}$ to describe this second-order reaction. Later,

Table 2 Summary of the thermodynamic parameters in the Co-Cu-Sn ternary system obtained in the present work

Phases	Parameters	References
Liquid	$(Co,Cu,Sn)_1$	
	${}^0L^{liquid}_{Co,Cu} = 31500 - 1.3T$	Ref 18
	${}^1L^{liquid}_{Co,Cu} = -595$	Ref 18
	${}^2L^{liquid}_{Co,Cu} = 3700$	Ref 18
	${}^0L^{liquid}_{Co,Sn} = -111091 + 557.904T - 66.556343T\ln T$	Ref 20
		Ref 20
	${}^1L^{liquid}_{Co,Sn} = -44585.348 + 222.131T - 27.092377T\ln T$	
	${}^2L^{liquid}_{Co,Sn} = 2252$	Ref 20
	${}^0L^{liquid}_{Cu,Sn} = -9002.8 - 5.838T$	Ref 21
	${}^1L^{liquid}_{Cu,Sn} = -20100 + 3.637T$	Ref 21
	${}^2L^{liquid}_{Cu,Sn} = -10528$	Ref 21
	${}^0L^{liquid}_{Co,Cu,Sn} = 22871 - 37.221T$	This work
	${}^1L^{liquid}_{Co,Cu,Sn} = -91174 + 48.319T$	This work
	${}^2L^{liquid}_{Co,Cu,Sn} = 90575 - 148.991T$	This work
Fcc	$(Co,Cu,Sn)_1$	
	${}^0L^{Fcc}_{Co,Cu} = 34600 - 4.0T$	Ref 18
	${}^1L^{Fcc}_{Co,Cu} = -6410 + 3.7T$	Ref 18
	${}^2L^{Fcc}_{Co,Cu} = 4390$	Ref 18
	${}^0TC^{Fcc}_{Co,Cu} = 812$	Ref 18
	${}^0L^{Fcc}_{Co,Sn} = -13699 + 15.965T$	Ref 20
	${}^0TC^{Fcc}_{Co,Sn} = -1721$	Ref 20
	${}^0L^{Fcc}_{Cu,Sn} = -8128 + 0.962T$	Ref 22
	${}^1L^{Fcc}_{Cu,Sn} = -19369 + 7.250T$	Ref 22
	${}^0L^{Fcc}_{Co,Cu,Sn} = 84580$	This work
Bcc	$(Co,Cu,Sn)_1$	
	${}^0L^{Bcc}_{Co,Cu} = 30000$	Ref 18
	${}^0L^{Bcc}_{Cu,Sn} = -44822 + 51.216$	Ref 21
	${}^1L^{Bcc}_{Cu,Sn} = -6877 - 56.427T$	Ref 21
Hcp	$(Co,Cu,Sn)_1$	
	${}^0L^{Hcp}_{Co,Cu} = 30000$	Ref 18
	${}^0L^{Hcp}_{Co,Sn} = 7000$	Ref 20
	${}^0L^{Hcp}_{Cu,Sn} = 5000$	Ref 21
Co_3Sn_2	$(Co,Cu,Sn)_1(Cu,Sn)_1(Co,Va)_{0.5}(Co,Va)_{0.5}$	
	$DG_{Co_2Sn} = -29681 DG_{CoSn} = -32054 + 13.505T$	Ref 20
	${}^0L_{Co_3Sn_2} = -18482\ {}^1L_{Co_3Sn_2} = +17048$	Ref 20
	${}^1W_{Co_3Sn_2} = -11000 + 9T\ {}^2W_{Co_3Sn_2} = 500$	Ref 20
		Ref 20
	$G^{Co_3Sn_2}_{Co:Sn:Co:Co} = 2{}^0G^{Hcp(Co)}_{Co} + {}^0G^{Bct(Sn)}_{Sn} + DG_{Co_2Sn}$	
		Ref 20
	$G^{Co_3Sn_2}_{Co:Sn:Co:Va} = G^{Co_3Sn_2}_{Co:Sn:Va:Co} = 1.5{}^0G^{Hcp(Co)}_{Co} + {}^0G^{Bct(Sn)}_{Sn} + 0.5DG_{Co_2Sn} + 0.5DG_{CoSn} + 0.25{}^0L_{Co_3Sn_2} + {}^1W_{Co_3Sn_2}$	

Table 2 continued

Phases	Parameters	References
		Ref 20
	$G^{Co_3Sn_2}_{Co:Sn:Va:Va} = {}^0G^{Hcp(Co)}_{Co} + {}^0G^{Bct(Sn)}_{Sn} + DG_{CoSn}$	
		Ref 20
	$G^{Co_3Sn_2}_{Co:Sn:Co,Va:Co} = G^{Co_3Sn_2}_{Co:Sn:Co:Co,Va} = 0.25{}^0L_{Co_3Sn_2} + 0.375{}^1L_{Co_3Sn_2} - {}^1W_{Co_3Sn_2} + {}^2W_{Co_3Sn_2}$	
		Ref 20
	$G^{Co_3Sn_2}_{Co:Sn:Co,Va:Va} = G^{Co_3Sn_2}_{Co:Sn:Va:Co,Va} = 0.25{}^0L_{Co_3Sn_2} - 0.375{}^1L_{Co_3Sn_2} - {}^1W_{Co_3Sn_2} - {}^2W_{Co_3Sn_2}$	
		Ref 20
	${}^1L^{Co_3Sn_2}_{Co:Sn:Co,Va:Co} = {}^1L^{Co_3Sn_2}_{Co:Sn:Co:Co,Va} = {}^1L^{Co_3Sn_2}_{Co:Sn:Co,Va:Va} = {}^1L^{Co_3Sn_2}_{Co:Sn:Va:Co,Va} = 0.125{}^1L_{Co_3Sn_2} - {}^2W_{Co_3Sn_2}$	
		This work
	$G^{Co_3Sn_2}_{Cu:Sn:Va:Va} = {}^0G^{Fcc(Cu)}_{Cu} + {}^0G^{Bct(Sn)}_{Sn} + 37163 - 29.864T$	
		This work
	$G^{Co_3Sn_2}_{Cu:Sn:Co:Co} = {}^0G^{Hcp(Co)}_{Co} + {}^0G^{Fcc(Cu)}_{Cu} + {}^0G^{Bct(Sn)}_{Sn} + 4293 - 19.969T$	
		This work
	$G^{Co_3Sn_2}_{Cu:Sn:Va:Co} = G^{Co_3Sn_2}_{Cu:Sn:Co:Va} = 0.5{}^0G^{Hcp(Co)}_{Co} + {}^0G^{Fcc(Cu)}_{Cu} + {}^0G^{Bct(Sn)}_{Sn} - 47386 + 20.055T$	
		This work
	${}^0L^{Co_3Sn_2}_{Cu:Sn:Co,Va:Va} = {}^0L^{Co_3Sn_2}_{Cu:Sn:Va:Co,Va} = 142700 + 39.940T$	
		This work
	${}^1L^{Co_3Sn_2}_{Cu:Sn:Co,Va:Va} = {}^1L^{Co_3Sn_2}_{Cu:Sn:Va:Co,Va} = -163728 + 5.0T$	
		This work
	${}^2L^{Co_3Sn_2}_{Cu:Sn:Co,Va:Va} = {}^2L^{Co_3Sn_2}_{Cu:Sn:Va:Co,Va} = -103022 - 5.0T$	
		This work
	$L^{Co_3Sn_2}_{Cu:Sn:Co,Va:Co,Va} = -882393$	
CoSn	$(Co,Cu)_1(Sn)_1$	
		Ref 20
	$G^{CoSn}_{Co:Sn} = {}^0G^{Hcp(Co)}_{Co} + {}^0G^{Bct(Sn)}_{Sn} - 41800 + 11.788T$	
$CoSn_3$	$(Co,Cu)_1(Sn)_3$	
		Ref 19
	$G^{CoSn_3}_{Co:Sn} = {}^0G^{Hcp(Co)}_{Co} + 3{}^0G^{Bct(Sn)}_{Sn} - 62800 + 16.397T$	
		This work
	$G^{CoSn_3}_{Cu:Sn} = {}^0G^{Fcc(Cu)}_{Cu} + 3{}^0G^{Bct(Sn)}_{Sn} + 4000$	
		This work
	${}^0L^{Co_3Sn}_{Co,Cu:Sn} = -19311$	

Table 2 continued

Phases	Parameters	References
$CoSn_2$	$(Co,Cu)_1(Sn)_2$	
		Ref 19
	$G^{CoSn_2}_{Co:Sn} = {}^0G^{Hcp(Co)}_{Co} + 2{}^0G^{Bct(Sn)}_{Sn} - 34425 + 5.790T$	
		This work
	$G^{CoSn_2}_{Cu:Sn} = {}^0G^{Fcc(Cu)}_{Cu} + 2{}^0G^{Bct(Sn)}_{Sn} + 3000$	
	${}^0L^{CoSn_2}_{Co,Cu:Sn} = -11663$	This work
$Cu_{10}Sn_3$	$(Cu,Co)_{10}(Sn)_3$	
		Ref 21
	$G^{Cu_{10}Sn_3}_{Cu:Sn} = 10{}^0G^{Fcc(Cu)}_{Cu} + 3{}^0G^{Bct(Sn)}_{Sn} - 86515 - 18.828T$	
Cu_3Sn	$(Cu,Co)_3(Sn)_1$	
		Ref 21
	$G^{Cu_3Sn}_{Cu:Sn} = 3{}^0G^{Fcc(Cu)}_{Cu} + {}^0G^{Bct(Sn)}_{Sn} - 3277 - 0.817T$	
		This work
	$G^{Cu_3Sn}_{Co:Sn} = 3{}^0G^{Hcp(Co)}_{Co} + {}^0G^{Bct(Sn)}_{Sn} - 4000$	
		This work
$Cu_{41}Sn_{11}$	$(Cu,Co)_{10}(Sn)_3$	
		Ref 21
	$G^{Cu_{41}Sn_{11}}_{Cu:Sn} = 41{}^0G^{Fcc(Cu)}_{Cu} + 11{}^0G^{Bct(Sn)}_{Sn} - 328822 - 66.602T$	
αCu_6Sn_5	$(Co,Cu)_6(Sn)_5$	
		Ref 21
	$G^{\beta Cu_6Sn_5}_{Co:Sn} = 6{}^0G^{Hcp(Co)}_{Co} + 5{}^0G^{Bct(Sn)}_{Sn} - 78427 + 4.465T$	
βCu_6Sn_5	$(Co,Cu)_6(Sn)_5$	
		Ref 21
	$G^{\beta Cu_6Sn_5}_{Cu:Sn} = 6{}^0G^{Fcc(Cu)}_{Cu} + 5{}^0G^{Bct(Sn)}_{Sn} - 75565 - 1.748T$	
		This work
	$G^{\beta Cu_6Sn_5}_{Co:Sn} = 6{}^0G^{Hcp(Co)}_{Co} + 5{}^0G^{Bct(Sn)}_{Sn} - 22000$	
	${}^0L^{\beta Cu_6Sn_5}_{Co,Cu:Sn} = -501479 + 330T$	This work
$D0_3(Cu_3Sn)$	$(Co,Cu)_3(Co,Cu)_1$	
		Ref 21
	$G^{D0_3(Cu_3Sn)}_{Cu:Cu} = 4{}^0G^{Bcc(Cu)}_{Cu} = 4{}^0G^{Fcc(Cu)}_{Cu} + 16068 - 5.02T$	
		Ref 21
	$G^{D0_3(Cu_3Sn)}_{Cu:Sn} = 3{}^0G^{Fcc(Cu)}_{Cu} + {}^0G^{Bct(Sn)}_{Sn} - 23668 - 9.754T$	
		Ref 21
	$G^{D0_3(Cu_3Sn)}_{Sn:Cu} = {}^0G^{Fcc(Cu)}_{Cu} + 3{}^0G^{Bct(Sn)}_{Sn} + 483916$	

Table 2 continued

Phases	Parameters	References
	$G_{Sn:Sn}^{D0_3(Cu_3Sn)} = 4^0G_{Sn}^{Bcc(Sn)} = 4^0G_{Sn}^{Bct(Sn)} + 17600 - 24T$	Ref 21
	${}^0L_{Cu:Cu,Sn}^{D0_3(Cu_3Sn)} = -7431 - 10.124T$	Ref 21
	${}^1L_{Cu:Cu,Sn}^{D0_3(Cu_3Sn)} = 11.958T$	Ref 21
	${}^0L_{Cu,Sn:Sn}^{D0_3(Cu_3Sn)} = 183400 - 168.876T$	Ref 21
$Co_2Cu_8Sn_3$	$(Co)_2(Cu)_{7.5}(Sn)_3$	This work
	$G_{Co:Cu:Sn}^{Co_2Cu_8Sn_3} = 2^0G_{Co}^{Hcp(Co)} + 7.5^0G_{Cu}^{Fcc(Cu)} + 3^0G_{Sn}^{Bct(Sn)} - 102954 - 22.161T$	

Dong et al.[53] adjusted the decomposition temperature of $Cu_{41}Sn_{11}$ in the assessment of the Au-Cu-Sn ternary system based on the result determined by Li et al.[52] To avoid the appearance of Fcc in a high-order system in the composition range far from its homogeneity range, Wang et al.[22] modified the interaction parameters for the Fcc phase. Therefore, the parameters obtained by Shim et al.[21] and modified by Wang et al.[22] are adopted in this work.

2.4 The Co-Cu-Sn Ternary System

The isothermal sections of the Co-Cu-Sn ternary system were measured by Chen et al.[16] using the equilibrium alloys method at 1273, 1073 and 523K. However, some phase relations are not certain at 523K because of the high melting point of Co and Cu. The solubilities of Cu in $CoSn_3$, Co_3Sn_2 and $CoSn_2$, and the solubility of Co in βCu_6Sn_5 were measured. In addition, a ternary compound, $Co_2Cu_8Sn_3$, has been found at 1073K, which does not exist at 1273 and 523K. It has also been reported that $Co_2Cu_8Sn_3$ has a simple cubic structure and lattice constant of 17.9 Å without specific crystal structure.[16]

Using the DSC (Differential Scanning Calorimetry) method, the heating curves and cooling curves of alloys $(Co_{0.5}Cu_{0.5})_{100-x}Sn_x$ (x=10, 20, 30, 40 and 50) were measured by Liu et al.[17] In addition, the primary phase and phase constitutions at room temperature are also reported by Liu et al.[17] According to the measurement, the primary phase is Fcc(Co) when x is equal to 10 or 20 and Co_3Sn_2 when x is equal to 30, 40 or 50. The phase relationships were also determined by Liu et al.[17] However, they found four-phase regions at room temperature. Considering that a non-equilibrium state is created because of the rapid cooling rate and the high melting-point of Co and Cu, only the primary phase information and the DSC data above 700K are used in the present work.

3 Thermodynamic Models

3.1 Unary Phase

The Gibbs energy function ${}^0G_i(T)$ for the pure elements i, i.e. Co, Cu and Sn, are expressed as:

$${}^0G_i = a + bT + cT\ln T + dT^2 + eT^{-1} + fT^3 + gT^7 + hT^{-9} \quad \text{(Eq 1)}$$

where T is the absolute temperature and a to h are coefficients. In the present modeling, the values of a to h are taken from the SGTE compilation by Dinsdale.[41]

3.2 Solution Phase

The Gibbs energy of the solution phases, i.e. liquid, Fcc, Bcc and Hcp, are described by the Redlich-Kister polynomial[42]:

$$\begin{aligned} G_{Co,Cu,Sn}^{\varphi} =& x_{Co}^0G_{Co}^{\varphi} + x_{Cu}^0G_{Cu}^{\varphi} + x_{Sn}^0G_{Sn}^{\varphi} + RT[x_{Co}\ln(x_{Co}) + x_{Cu}\ln(x_{Cu}) + x_{Sn}\ln(x_{Sn})] \\ &+ x_{Co}x_{Cu}({}^0L_{Co,Cu}^{\varphi} + {}^1L_{Co,Cu}^{\varphi}(x_{Co} - x_{Cu}) + {}^2L_{Co,Cu}^{\varphi}(x_{Co} - x_{Cu})^2) \\ &+ x_{Cu}x_{Sn}({}^0L_{Cu,Sn}^{\varphi} + {}^1L_{Cu,Sn}^{\varphi}(x_{Cu} - x_{Sn}) + {}^2L_{Cu,Sn}^{\varphi}(x_{Cu} - x_{Sn})^2) \\ &+ x_{Co}x_{Sn}({}^0L_{Co,Sn}^{\varphi} + {}^1L_{Co,Sn}^{\varphi}(x_{Co} - x_{Sn}) + {}^2L_{Co,Sn}^{\varphi}(x_{Co} - x_{Sn})^2) \\ &+ x_{Co}x_{Cu}x_{Sn}(x_{Co}^0L_{Co,Cu,Sn}^{\varphi} + x_{Cu}^1L_{Co,Cu,Sn}^{\varphi} + x_{Sn}^2L_{Co,Cu,Sn}^{\varphi}) \end{aligned} \quad \text{(Eq 2)}$$

where φ is the solution phase. R is the gas content. ${}^0G_{Co}^{\varphi}$, ${}^0G_{Cu}^{\varphi}$ and ${}^0G_{Sn}^{\varphi}$ are the Gibbs energies for pure Co, Cu and

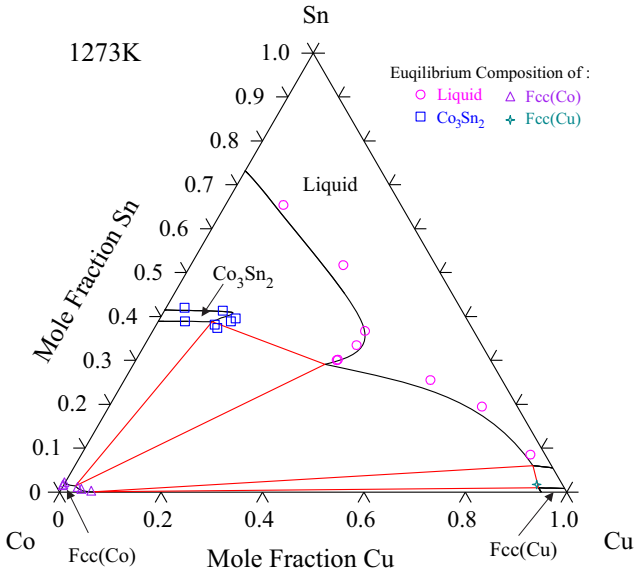

Fig. 2 The calculated isothermal section of the Co-Cu-Sn ternary system at 1273K

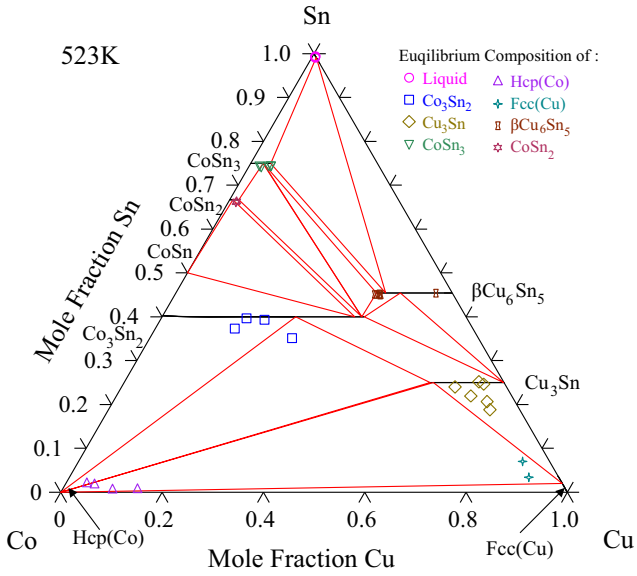

Fig. 4 The calculated isothermal section of the Co-Cu-Sn ternary system at 523K

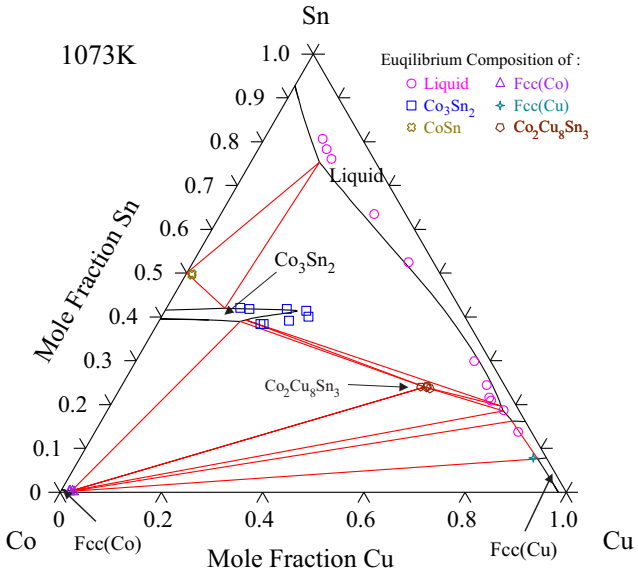

Fig. 3 The calculated isothermal section of the Co-Cu-Sn ternary system at 1073K

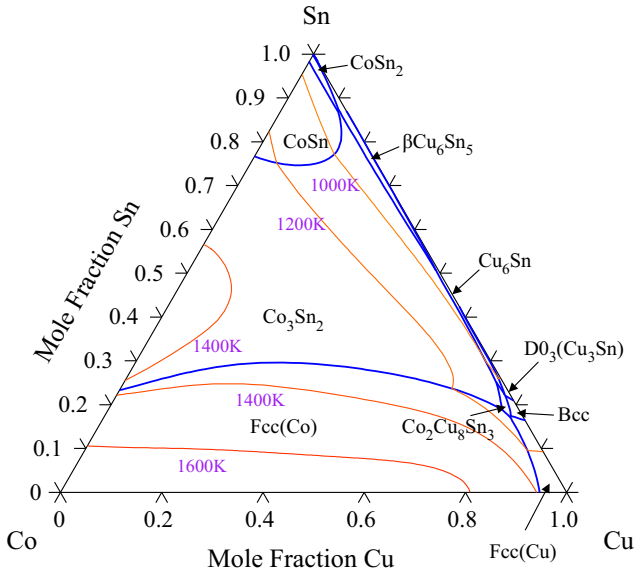

Fig. 5 The calculated liquidus projection for the Co-Cu-Sn ternary system. The blue solid lines are the monovariant liquidus lines and the red lines represent the composition of liquidus at different temperatures

Sn at the standard element reference state. For example, the reference states for Co, Cu and Sn are Liquid(Co), Liquid(Cu) and Liquid(Sn) respectively, where φ represents the liquid phase. These parameters are also taken from the SGTE database.[41] x_{Co}, x_{Cu} and x_{Sn} are the mole fractions for Co, Cu and Sn, respectively. ${}^{v}L^{\varphi}_{i,j}$ (i, j, k = Co, Cu and Sn) are interaction parameters from the binary system and ${}^{v}L^{\varphi}_{i,j,k}$ are interaction parameters from the ternary system. In addition, the interaction parameters can be described by:

$$L = a + bT \quad \text{(Eq 3)}$$

where a and b are constants to be evaluated.

3.3 Intermetallic Compounds

The two-sublattice model, $(Co,Cu)_m(Sn)_n$, is used to describe the binary line compounds which extend into the ternary system, i.e. $CoSn_3$, $CoSn_2$, Cu_3Sn and βCu_6Sn_5.

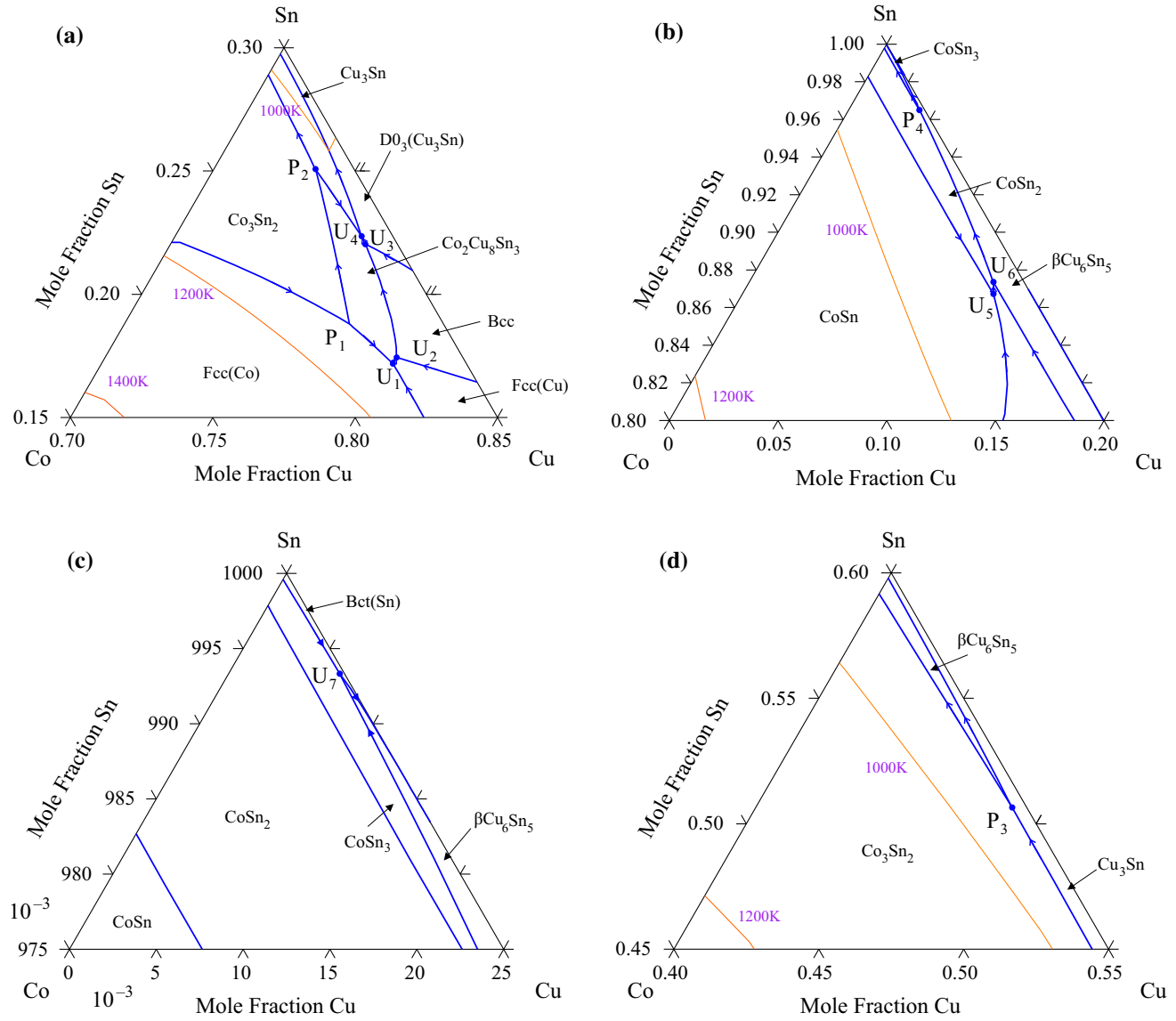

Fig. 6 Enlarged views of the liquidus projection (a) 70-85 at.% Cu, 15-30 at.% Sn; (b) 0-20 at.% Cu, 80-100 at.% Sn; (c) 0-2.5 at.% Cu, 97.5-100 at.% Sn; (d) 40-55 at.% Cu, 45-60 at.% Sn. The blue solid lines are the monovariant liquidus lines and the red lines represent the composition of liquidus at different temperatures. The arrows on the monovariant liquidus lines show the direction of decreasing temperature (Color figure online)

The Gibbs energy per mole formula of $CoSn_3$ can be expressed as follow:

$$G^{CoSn_3} = y'_{Co} G^{CoSn_3}_{Co:Sn} + y'_{Cu} G^{CoSn_3}_{Cu:Sn} + 3RT(y'_{Co} \ln y'_{Co} + y'_{Cu} \ln y'_{Cu}) + y'_{Co} y'^{0}_{Cu} L^{CoSn_3}_{Co,Cu:Sn} \quad \text{(Eq 4)}$$

where y'_{Co} and y'_{Cu} are the site fractions of Co and Cu on the first sub-lattice, respectively. Analogous expressions are used to describe the Gibbs energies of the $CoSn_3$, $CoSn_2$, and βCu_6Sn_5 phases.

The four-sublattice model, $(Co,Sn)_1(Sn)_1(Co,Va)_{0.5}(Co,Va)_{0.5}$, was employed to describe the Co_3Sn_2 phase by Dong et al.[19] In the present work, this model is modified as $(Co,Cu,Sn)_1(Cu,Sn)_1(Co,Va)_{0.5}(Co,Va)_{0.5}$ to describe the solubility of Cu in the Co_3Sn_2 phase. The Gibbs energy of Co_3Sn_2 can be expressed as follow:

Table 3 Invariant reactions calculated in the Co-Cu-Sn ternary system

Reaction	T(K)	x(Co)	x(Cu)	x(Sn)	Reaction type
Liquid + Co_3Sn_2 + Fcc(Co) ↔ $Co_2Cu_8Sn_3$	1075.3	0.033	0.779	0.188	P_1
Liquid + Fcc(Co) ↔ Fcc(Cu) + $Co_2Cu_8Sn_3$	1057.9	0.026	0.802	0.172	U_1
Liquid + Fcc(Cu) ↔ Bcc(A2) + $Co_2Cu_8Sn_3$	1053.8	0.023	0.802	0.175	U_2
Liquid + $Co_2Cu_8Sn_3$ + Co_3Sn_2 ↔ Cu_3Sn	1019.3	0.014	0.736	0.251	P_2
Liquid + Bcc(A2) ↔ $Co_2Cu_8Sn_3$ + $D0_3(Cu_3Sn)$	1016.8	0.011	0.769	0.220	U_3
Liquid + $Co_2Cu_8Sn_3$ ↔ Cu_3Sn + $D0_3(Cu_3Sn)$	1015.1	0.011	0.766	0.223	U_4
Liquid + Co_3Sn_2 + Cu_3Sn ↔ βCu_6Sn_5	871.4	0.005	0.488	0.506	P_3
Liquid + CoSn ↔ Co_3Sn_2 + $CoSn_2$	809.9	0.017	0.115	0.867	U_5
Liquid + Co_3Sn_2 ↔ βCu_6Sn_5 + $CoSn_2$	792.3	0.014	0.112	0.874	U_6
Liquid + βCu_6Sn_5 + $CoSn_2$ ↔ $CoSn_3$	640.2	0.002	0.033	0.965	P_4
Liquid + CoSn$_3$ ↔ βCu_6Sn_5 + Bct(Sn)	503.1	<0.001	0.006	0.994	U_7

$$
\begin{aligned}
G^{Co_3Sn_2} = & \sum_i \sum_j \sum_k \sum_l y_i' y_j'' y_k''' y_l'''' G_{i:j:k:l} \\
& + RT\Big(\sum_i y_i' \ln y_i' + \sum_j y_j'' \ln y_j'' \\
& + 0.5 \sum_k y_k''' \ln y_k''' + 0.5 \sum_l y_l'''' \ln y_l''''\Big) \\
& + \sum_i \sum_{p>i} \sum_j \sum_k \sum_l y_i' y_p' y_j'' y_k''' y_l'''' L_{i,p:j:k:l} \\
& + \sum_i \sum_j \sum_{p>j} \sum_k \sum_l y_i' y_j'' y_p'' y_k''' y_l'''' L_{i:j,p:k:l} \\
& + \sum_i \sum_j \sum_k \sum_{p>k} \sum_l y_i' y_j'' y_k''' y_p''' y_l'''' L_{i:j:k,p:l} \\
& + \sum_i \sum_j \sum_k \sum_l \sum_{l>k} y_i' y_j'' y_k''' y_l'''' y_p'''' L_{i:j:k::,p} \\
& + \sum_i \sum_{p>i} \sum_j \sum_{q>j} \sum_k \sum_l y_i' y_p' y_j'' y_q'' y_k''' y_l'''' L_{i,p:j,q:k:l} \\
& + \sum_i \sum_{p>i} \sum_j \sum_q \sum_{q>k} \sum_l y_i' y_p' y_j'' y_k''' y_q''' y_l'''' L_{i,p:j:k,q:l} \\
& + \sum_i \sum_{p>i} \sum_j \sum_k \sum_q \sum_{q>l} y_i' y_p' y_j'' y_k''' y_l'''' y_q'''' L_{i,p:j:k:l,q} \\
& + \sum_i \sum_j \sum_{p>j} \sum_k \sum_{q>k} \sum_l y_i' y_j'' y_p'' y_k''' y_q''' y_l'''' L_{i:j,p:k,q:l} \\
& + \sum_i \sum_j \sum_{p>j} \sum_k \sum_l \sum_{q>l} y_i' y_j'' y_k''' y_p''' y_l'''' y_q'''' L_{i:j,p:k:l,q} \\
& + \sum_i \sum_j \sum_k \sum_{p>k} \sum_l \sum_{q>l} y_i' y_j'' y_k''' y_p''' y_l'''' y_q'''' L_{i:j,p:k:l,q}
\end{aligned}
\qquad \text{(Eq 5)}
$$

where y_i', y_j'', y_k''' and y_l'''' are the site fractions of components i, j, k and l (i = Co, Cu or Sn; j = Cu or Sn; k = Co or Va; l = Co or Va) on the first, second, third and fourth-lattice, respectively.

Because the calculated composition of $Co_2Cu_8Sn_3$ should be closer to the values measured by Chen et al.,[16] the model $(Co)_2(Cu)_{7.5}(Sn)_3$ is used to describe the $Co_2Cu_8Sn_3$ phase. In addition, the measured solid solubility of this ternary compound is small. Thus, the stoichiometric model, $(Co)_2(Cu)_{7.5}(Sn)_3$, was used to describe this compound. The Gibbs energy of $Co_2Cu_8Sn_3$ per mole formula unit can be expressed as:

$$G^{Co_2Cu_8Sn_3} = 2^0G_{Co}^{Bcp(Co)} + 7.5^0G_{Cu}^{Fcc(Cu)} + 3^0G_{Sn}^{Bct(Sn)} + a + bT \qquad \text{(Eq 6)}$$

where ${}^0G_{Co}^{Hcp(Co)}$, ${}^0G_{Cu}^{Fcc(Cu)}$ and ${}^0G_{Sn}^{Bct(Sn)}$ are the Gibbs energies for Co, Cu and Sn at their standard element reference state respectively. a and b are parameters which are to be evaluated in this work.

4 Results and Discussion

The thermodynamic parameters and models obtained in the present work are listed in Table 2, with J/molas the unit of the Gibbs energy.

The formation enthalpy of $Co_2Cu_8Sn_3$ has not been measured in previous literature. In addition, it is difficult to calculate the formation enthalpy using first-principles calculations because the site occupancy of atoms and space group of $Co_2Cu_8Sn_3$ are unknown. For these reasons, the formation enthalpy of $Co_2Cu_8Sn_3$ is only evaluated using the CALPHAD methods[54] in this work. In addition, considering the marked difference between the formation enthalpies obtained from experimental and first-principles methods,[55–58] the formation enthalpies of end-members, i.e. $G_{Cu:Sn}^{CoSn_3}$, $G_{Co:Sn}^{CoSn_2}$, $G_{Co:Sn}^{\beta Cu_6Sn_5}$ and $G_{Co:Sn}^{Cu_3Sn}$ are estimated. The temperature dependence parameters of ${}^0L_{Cu:Sn}^{\beta Cu_6Sn_5}$ are set to arbitrary values, as only one experimental isothermal section contains these phases.

4.1 Isothermal Sections

Figure 2, 3 and 4 shows the calculated isothermal sections at 1273, 1073 and 523K of the Co-Cu-Sn ternary system over the whole composition range, with the equilibrium compositions measured by Chen et al.[16] The experimental

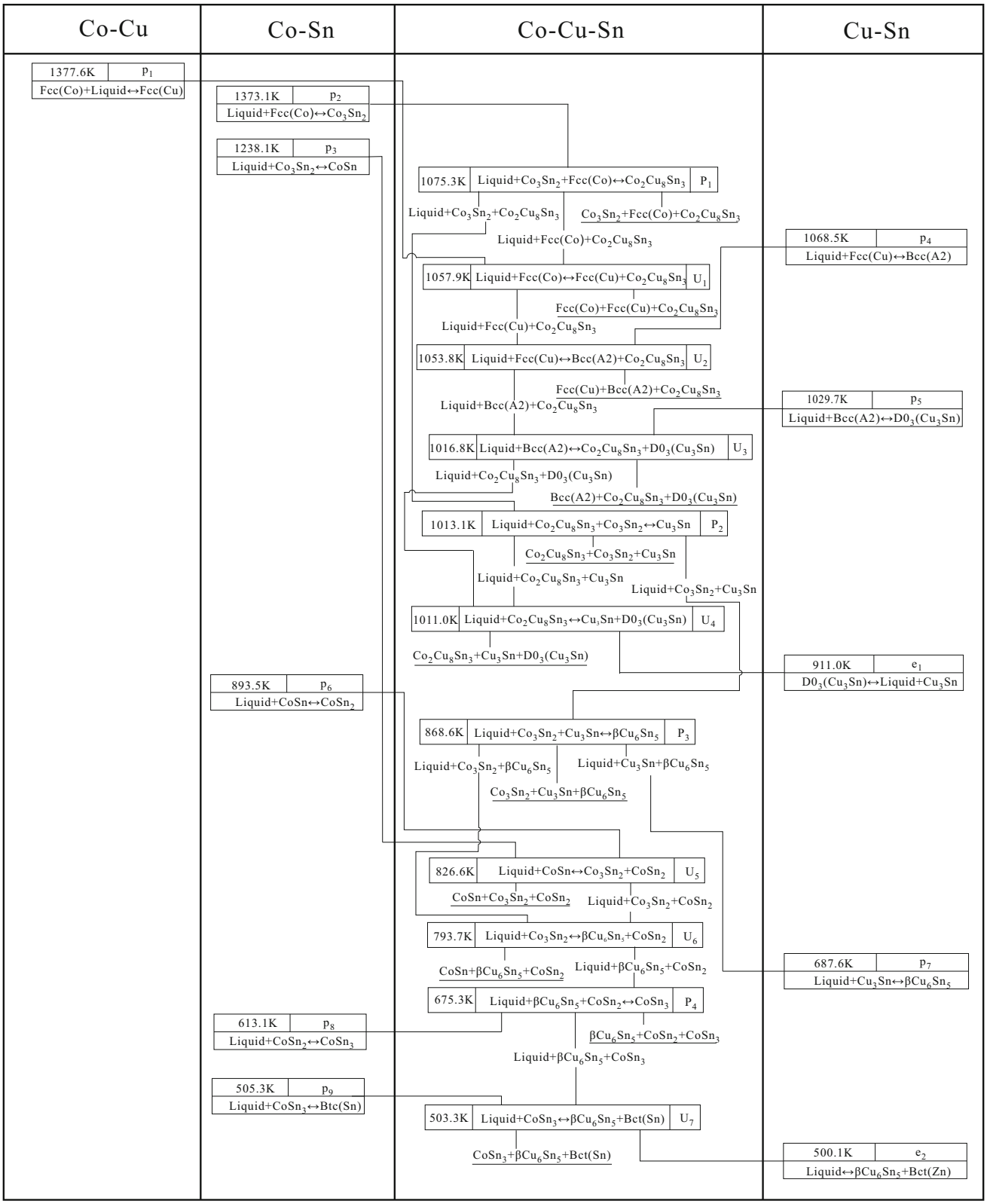

Fig. 7 The reaction scheme for the Co-Cu-Sn ternary system according to the present thermodynamic description

equilibrium composition of each phase is shown by different symbols and colors. The calculated isothermal sections agree well with the measured ones.

The calculated 1273K section is shown in Fig. 2. The liquidus shows a tip at 37.78 at.% Cu and 29.12 at.% Sn. Fcc(Co) and Fcc(Cu) show small solid solubilities. These phenomena are consistent with the experimental results.

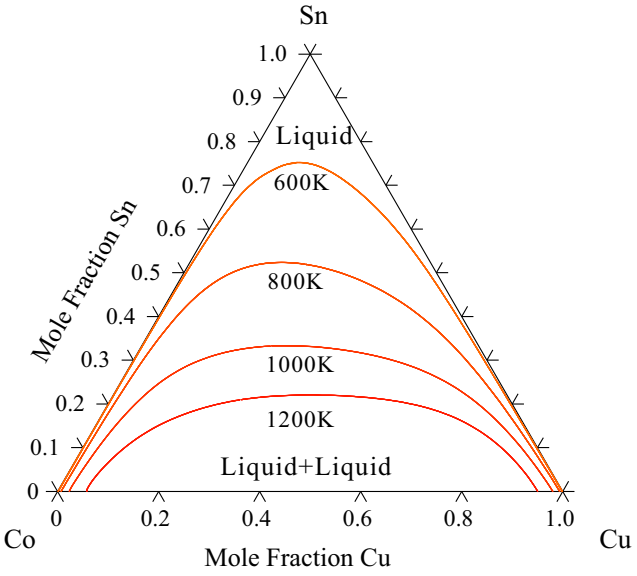

Fig. 8 The boundaries of the liquidus miscibility gap of the Co-Cu-Sn ternary system calculated at different temperatures

The calculated 1073K isothermal section is shown in Fig. 3. As can be seen, most of the experimental data can be described by the present calculation. The calculation reproduced a narrow liquid+Co_3Sn_2+$Co_2Cu_8Sn_3$ three-phase region and the tip of the liquidus at 1273K has diasappeared.

Figure 4 presents the calculated isothermal section at 523K. The experimental data show a large solid solubility for Hcp(Co), Fcc(Cu), Cu_3Sn and Co_3Sn_2, which may attributed to the samples being not fully equilibrated.[16] Therefore, Cu_3Sn and Co_3Sn_2 are seen as line compounds in the present work, and it is considered that Co and Cu have small solid solubility. The CoSn phase is not assessed because of the insignificant solid solubilities. The calculated solid solubilities of βCu_6Sn_5 and $CoSn_3$ are in good agreement with the measurement. In addition, the calculated phase regions in the Sn-rich part are different from the reported ones.[16] In the present calculation, the equilibrium composition of Co_3Sn_2 in many phase regions, including CoSn+$CoSn_2$+Co_3Sn_2, CoSn+$CoSn_2$+Co_3Sn_2 and $CoSn_2$+Co_3Sn_2, contains more Cu than that predicted by Chen et al.[16]

4.2 Liquidus Projection

Figure 5 shows the liquidus projection for the Co-Cu-Sn ternary system, in which the nonvariant reactions are drawn using blue solid lines and the liquidus at different

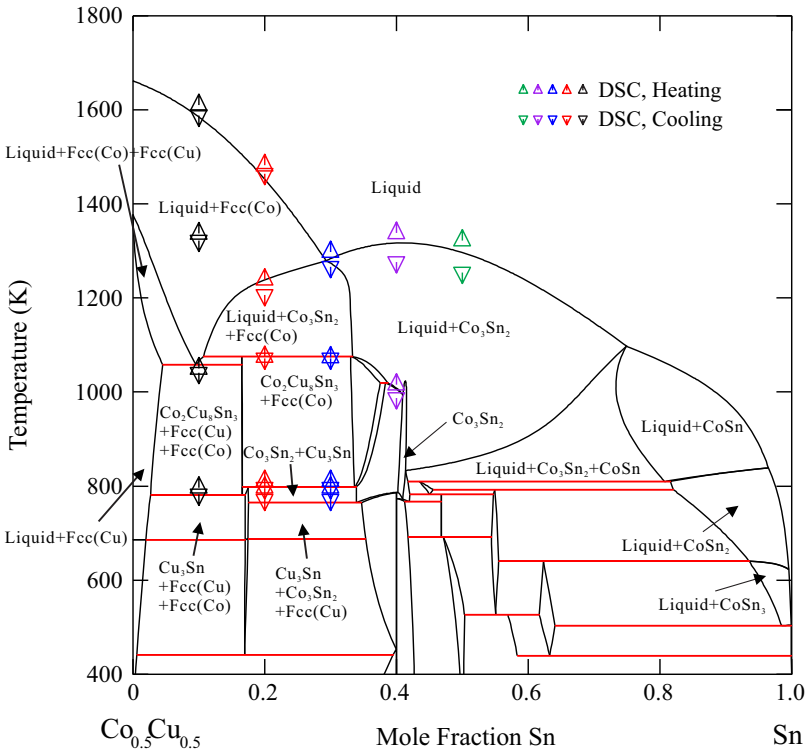

Fig. 9 The calculated vertical section $Co_{0.5}Cu_{0.5}$-Sn, compared with the experimental values from the literature[17]

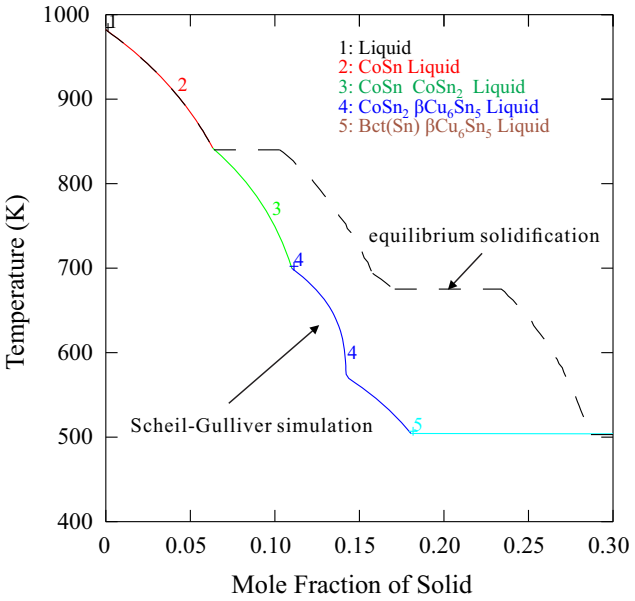

Fig. 10 Evolution of the fraction of the solid phase of $Co_5Cu_5Sn_{90}$ according to the Scheil-Gulliver simulation

temperatures are drawn using red solid lines. It is characterized by eleven invariant reactions, including four peritectic reactions and seven transition reactions. No eutectic reaction was found. The enlarged views of the liquidus projection are listed in Fig. 6(a)-(d). The calculated temperature and compositions of each invariant equilibrium is listed in Table 3. Figure 7 presents the calculated reaction scheme for the Co-Cu-Sn ternary system.

It can be observed that the temperatures of reactions Liquid + $Co_2Cu_8Sn_3 + Co_3Sn_2 \leftrightarrow Cu_3Sn$ and Liquid + $Co_3Sn_2 + Cu_3Sn \leftrightarrow \beta Cu_6Sn_5$ are higher than the melting points of Cu_3Sn and βCu_6Sn_5, respectively. It is difficult to adjust the temperature dependence parameters to avoid this situation. This result can be attributed to the fact that the melting point of Co (1768.1K) is higher than that of Cu (1382.8K) and the melting points of Cu_3Sn_2 and βCu_6Sn_5 may be increased by doping Cu.

The calculated boundaries of the liquidus miscibility gap of the Co-Cu-Sn ternary system at 1200, 1000, 800 and 600K are shown in Fig. 8.

The liquid phase decomposes into the Co-rich phase and Cu-rich phase when the melt is undercooled below the liquidus surface. It can also be seen that the demixing temperature decreases with increasing Sn and it can be inferred that the liquid demixing in the Co-Cu binary system can be avoided by Sn addition.

4.3 Vertical Section and Scheil Solidification

The vertical section at $Co_{0.5}Cu_{0.5}$-Sn is shown in Fig. 9, compared with the phase transform temperature measured by Liu et al.[17] It can be seen that numerous experimental data can be described well by the present work. It is worth mentioning that the experimental liquidus temperatures[17] are not utilized during the evaluation of model parameters and are only used to validate the obtained thermodynamic description. However, the predicted liquidus temperatures are 1585, 1453, 1283, 1317 and 1297K at 10, 20, 30, 40 and 50 at.% Sn, respectively, which can well reproduce experimental temperautres obtained by cooling (1588 and 1464K at 10 and 20 at.% Sn, respectively) and heating (1297, 1338 and 1322K at 30, 40 and 50 at.% Sn, respectively).[17] Some phase transformation temperatures are also reproduced well, including Liquid + Co_3Sn_2 + Fcc(Co) $\leftrightarrow Co_2Cu_8Sn_3$, Liquid + Fcc(Co) $\leftrightarrow Co_2Cu_8Sn_3$ + Fcc(Cu) etc. In addition, the primary phase data are consistent with the experimental ones. However, there exists no phase transformation in the calculated section at approximately 1330K when the mole fraction of Sn is equal to 0.1. This point corresponds to a very weak peak on the heating and cooling curves.[17] Therefore, this situation is attributable to the magnetic transformation of Fcc(Co).

Figure 10 exhibits the variation in the fraction of the solid phase with temperature calculated in the present work, in which solid lines represent the Scheil-Gulliver simulation and the dashed lines represent the equilibrium solidification. For the simulation, $Co_5Cu_5Sn_{90}$ was chosen as the original composition.

5 Conclusion

Based on the thermodynamic description of the Co-Cu, Co-Sn and Cu-Sn binary systems and experimental phase equilibrium data for the Co-Cu-Sn ternary system reported in the literature, the thermodynamic parameters of the Co-Cu-Sn ternary system were evaluated. The calculated isothermal sections at 1273 and 1073K agree well with the experimental data. At 523K, the calculated equilibrium composition of Co_3Sn_2 in $CoSn+CoSn_2+Co_3Sn_2$, $CoSn+CoSn_2+Co_3Sn_2$ and $CoSn_2+Co_3Sn_2$, contains more Cu than the result reported in the literature. In addition, the liquidus projection has been calculated and no eutectic reaction was found. The effect of Sn addition on the liquid-liquid phase separation was also investigated.

Acknowledgment The financial supports from the National Natural Science Foundation of China (Nos. 52171024 and 51871186) and the National Key Research and Development Program of China (Materials Genome Initiative: 2017YFB0701700) are gratefully acknowledged. The authors thank the support from the High-Performance Computing Center of Central South University.

References

1. M.S. Węglowski, S. Błacha, and A. Phillips, Electron Beam Welding – Techniques and Trends – Review, *Vacuum*, 2016, **130**, p 72–92. https://doi.org/10.1016/j.vacuum.2016.05.004
2. H. Kuroki, K. Nezaki, T. Wakabayashi, and K. Nakamura, Application of Linear Friction Welding Technique to Aircraft Engine Parts, *IHI Engineering Reviews*, 2014, **47**, p 40–43.
3. A. Anand, and A. Khajuria, Welding Processes in Marine Application: A Review, *International Journal of Mechanical Engineering and Robotics Research*, 2015, **2**(1), p 215–225.
4. H.R. Kotadia, P.D. Howes, and S.H. Mannan, A Review: On the Development of Low Melting Temperature Pb-Free Solders, *Microelectron. Reliab.*, 2014, **54**(6–7), p 1253–1273. https://doi.org/10.1016/j.microrel.2014.02.025
5. S.F. Cheng, C.M. Huang, and M. Pecht, A Review of Lead-Free Solders for Electronics Applications, *Microelectron. Reliab.*, 2017, **75**, p 77–95. https://doi.org/10.1016/j.microrel.2017.06.016
6. N.C. Lee, Getting Ready for Lead-Free Solders, *Soldering and Surface Mount Technol*, 1997, **9**(2), p 65–69. https://doi.org/10.1108/09540919710800656
7. P. Sun, C. Andersson, X. Wei, Z. Cheng, Z. Lai, D. Shangguan, J. Liu. High temperature aging study of intermetallic compound formation of Sn-3.5Ag and Sn-4.0Ag-0.5Cu solders on electroless Ni (P) metallization; proceedings of the 56th Electronic Components and Technology Conference 2006, F, (2006). IEEE. https://doi/org/https://doi.org/10.1109/ECTC.2006.1645850
8. N. Dariavach, P. Callahan, J. Liang, and R. Fournelle, Intermetallic Growth Kinetics for Sn-Ag, Sn-Cu, and Sn-Ag-Cu Lead-Free Solders on Cu, Ni, and Fe-42Ni Substrates, *J. Electron. Mater.*, 2006, **35**(7), p 1581–1592. https://doi.org/10.1007/s11664-006-0152-7
9. F. Cheng, H. Nishikawa, and T. Takemoto, Microstructural and Mechanical Properties of Sn–Ag–Cu Lead-Free Solders with Minor Addition of Ni and/or Co, *J. Mater. Sci.*, 2008, **43**, p 3643–3648. https://doi.org/10.1007/s10853-008-2580-7
10. I.E. Anderson, B.A. Cook, J. Harringa, and R.L. Terpstra, Microstructural Modifications and Properties of Sn-Ag-Cu Solder Joints Induced by Alloying, *J. Electron. Mater.*, 2002, **31**(11), p 1166–1174. https://doi.org/10.1007/s11664-002-0006-x
11. Z.L. Ma, S.A. Belyakov, and C.M. Gourlay, Effects of Cobalt on the Nucleation and Grain Refinement of Sn-3Ag-0.5Cu Solders, *J. Alloys and Compound.*, 2016, **682**, p 326–337. https://doi.org/10.1016/j.jallcom.2016.04.265
12. M.G.M. Miranda, E. Estévez-Rams, G. Martinez, and M.N. Baibich, Phase Separation in $Cu_{90}Co_{10}$ High-Magnetoresistance Materials, *Phys. Rev. B*, 2003, **68**, p 1014434. https://doi.org/10.1103/PhysRevB.68.014434
13. T. Nishizawa, and K. Ishida, The Co−Cu (Cobalt-Copper) System, *Bull. Alloy Phase Diagram.*, 1984, **5**(2), p 161–165.
14. S. Curiotto, L. Battezzati, E. Johnson, and N. Pryds, Thermodynamics and Mechanism of Demixing in Undercooled Cu–Co–Ni Alloys, *Acta Mater.*, 2007, **55**(19), p 6642–6650.
15. Z.-K. Liu, Computational Thermodynamics and its Applications, *Acta Mater.*, 2020, **200**, p 745–792. https://doi.org/10.1016/j.actamat.2020.08.008
16. Y.K. Chen, C.M. Hsu, S.W. Chen, C.M. Chen, and Y.C. Huang, Phase Equilibria of Sn-Co-Cu Ternary System, *Metall. Mater. Trans. A.*, 2012, **43**(10), p 3586–3595. https://doi.org/10.1007/s11661-012-1192-7
17. J.M. Liu, W. Zhai, K. Zhou, D.L. Geng, and B.B. Wei, Thermophysical Properties and Liquid-Solid Transition Mechanisms of Ternary $(Co_{0.5}Cu_{0.5})(100–x)$ Snx Alloys, *Acta Physica Sinica*, 2016, **65**, p 22–228101. https://doi.org/10.7498/aps.65.228101
18. M. Palumbo, S. Curiotto, and L. Battezzati, Thermodynamic Analysis of the Stable and Metastable Co-Cu and Co-Cu-Fe Phase Diagrams, *Calphad*, 2006, **30**(2), p 171–178. https://doi.org/10.1016/j.calphad.2005.10.007
19. H.Q. Dong, S. Jin, L.G. Zhang, J.S. Wang, X.M. Tao, H.S. Liu, and Z.P. Jin, Thermodynamic Assessment of the Au-Co-Sn Ternary System, *J. Electron. Mater.*, 2009, **38**(10), p 2158–2169. https://doi.org/10.1007/s11664-009-0874-4
20. M. Jiang, J. Sato, I. Ohnuma, R. Kainuma, and K. Ishida, A Thermodynamic Assessment of the Co-Sn System, *Calphad*, 2004, **28**(2), p 213–220. https://doi.org/10.1016/j.calphad.2004.08.001
21. J.H. Shim, C.S. Oh, B.J. Lee, and D.N. Lee, Thermodynamic Assessment of the Cu-Sn System, *Int. J. Mater. Res.*, 1996, **87**(3), p 205–212. https://doi.org/10.1515/ijmr-1996-870310
22. J.A. Wang, C.L. Liu, C. Leinenbach, U.E. Klotz, P.J. Uggowitzer, and J.F. Loffler, Experimental Investigation and Thermodynamic Assessment of the Cu-Sn-Ti Ternary System, *Calphad*, 2011, **35**(1), p 82–94. https://doi.org/10.1016/j.calphad.2010.12.006
23. E.A. Owen, and D.M. Jones, Effect of Grain Size on the Crystal Structure of Cobalt, *Proceed. Phys. Soc. Sect. B*, 1954, **67**, p 456–466. https://doi.org/10.1088/0370-1301/67/6/302
24. H.W. King, Crystal Structures of the Elements at 25° C, *Bulletin of alloy phase diagrams*, 1981, **2**(3), p 401–402. https://doi.org/10.1007/BF02868307
25. H. Fjellvág, and A. Kjekshus, Structural Properties of Co_3Sn_2, Ni_3Sn_2 and Some Ternary Derivatives. Acta Chemica Scandinavica, *Series A: Phys. Inorgan. Chem.*, 1986, **40**, p 23–30.
26. A.K. Larsson, M. Haeberlein, S. Lidin, and U. Schwarz, Single Crystal Structure Refinement and High-Pressure Properties of CoSn, *J. Alloy. Compd.*, 1996, **240**(1–2), p 79–84. https://doi.org/10.1016/0925-8388(95)02189-2
27. M. Armbrüster, M. Schmidt, R. Cardoso-Gil, H. Borrmann, and Y. Grin, Crystal Structures of Iron Distannide, $FeSn_2$, and Cobalt Distannide, $CoSn_2$, *Zeitschrift für Kristallographie-New Crystal Structures*, 2007, **222**(2), p 83–84. https://doi.org/10.1524/ncrs.2007.0033
28. A. Lang, and W. Jeitschko, Two New Phases in the System Cobalt-tin: the Crystal Structures of α-and β-$CoSn_3$, *Z. Metallkd.*, 1996, **87**(10), p 759–764.
29. J.K. Brandon, W.B. Pearson, and D.J.N. Tozer, A Single-Crystal X-ray Diffraction Study of the ζ bronze Structure, $Cu_{20}Sn_6$, *Acta Crystallogr. Sect. B: Struct. Crystallogr. Cryst. Chem.*, 1975, **31**(3), p 774–779. https://doi.org/10.1107/S0567740875003780
30. M.H. Booth, J.K. Brandon, R.Y. Brizard, C.T. Chieh, and W.B. Pearson, γ-Brasses with F cells, *Acta Crystallogr. Sect. B: Struct. Crystallogr. Cryst. Chem.*, 1977, **33**(1), p 30–36. https://doi.org/10.1107/S0567740877002556
31. S. Fürtauer, D. Li, D. Cupid, and H. Flandorfer, The Cu–Sn Phase Diagram, Part I: New Experimental Results, *Intermetallics*, 2013, **34**, p 142–147.
32. Y. Watanabe, Y. Fujinaga, and H. Iwasaki, Lattice Modulation in the Long-Period Superstructure of Cu_3Sn, *Acta Crystallogr. B*, 1983, **39**(3), p 306–311. https://doi.org/10.1107/S0108768183002451
33. S. Lidin, and A.-K. Larsson, A Survey of Superstructures in Intermetallic NiAs-Ni_2In-type Phases, *J. Solid State Chem.*, 1995, **118**(2), p 313–322. https://doi.org/10.1006/jssc.1995.1350
34. A. Gangulee, G.C. Das, and M.B. Bever, An X-ray Diffraction and Calorimetric Investigation of the Compound Cu_6Sn_5, *Metallurgical Trans.*, 1973, **4**(9), p 2063–2066.
35. L. Kaufman, Coupled Phase Diagrams and Thermochemical Data for Transition Metal Binary Systems-III, *Calphad*, 1978, **2**(2), p 117–146. https://doi.org/10.1016/0364-5916(78)90031-7

36. M. Hasebe, and T. Nishizawa, Calculation of Phase Diagrams of the Iron-Copper and Cobalt-Copper Systems, *Calphad*, 1980, **4**(2), p 83–100. https://doi.org/10.1016/0364-5916(80)90026-7
37. J. Kubišta, and J. Vřešťál, Thermodynamics of the Liquid Co-Cu System and Calculation of Phase Diagram, *J. Phase Equilibria*, 2000, **21**(2), p 125–129. https://doi.org/10.1361/105497100770340165
38. M.A. Turchanin, and P.G. Agraval, Phase Equilibria and Thermodynamics of Binary Copper Systems with 3d-Metals v. Copper-Cobalt System, *Powder Metallurgy and Metal Ceram.*, 2007, **46**(1–2), p 77–89. https://doi.org/10.1007/s11106-007-0013-9
39. M.A. Turchanin, L.A. Dreval, A.R. Abdulov, and P.G. Agraval, Mixing Enthalpies of Liquid Alloys and Thermodynamic Assessment of the Cu-Fe-Co System, *Powder Metall. Met. Ceram.*, 2011, **50**(1–2), p 98–116. https://doi.org/10.1007/s11106-011-9307-z
40. Y. Yu, X.J. Liu, Z.P. Jiang, C.P. Wang, R. Kainuma, and K. Ishida, Thermodynamics and Liquid Phase Separation in the Cu–Co–Nb Ternary Alloys, *J. Mater. Res.*, 2011, **25**(9), p 1706–1717. https://doi.org/10.1557/JMR.2010.0223
41. A.T. Dinsdale, SGTE Data for Pure Elements, *Calphad*, 1991, **15**(4), p 317–425. https://doi.org/10.1016/0364-5916(91)90030-N
42. O. Redlich, and A. Kister, Algebraic Representation of Thermodynamic Properties and the Classification of Solutions, *Ind. Eng. Chem.*, 1948, **40**(2), p 345–348.
43. L.B. Liu, C. Andersson, and J. Liu, Thermodynamic Assessment of the Sn-Co Lead-Free Solder System, *J. Electron. Mater.*, 2004, **33**(9), p 935–939. https://doi.org/10.1007/s11664-004-0019-8
44. G.P. Vassilev, and K.I. Lilova, Contribution to the Thermodynamics of the Co-Sn System, *Arch. Metall. Mater.*, 2006, **51**(3), p 365–375.
45. V. Jedličková, A. Zemanová, and A. Kroupa, The Thermodynamic Assessment of the Co-Sn System, *J. Phase Equilib. Diffus.*, 2019, **40**(1), p 21–33. https://doi.org/10.1007/s11669-018-0687-3
46. K.W. Moon, W.J. Boettinger, U.R. Kattner, F.S. Biancaniello, and C.A. Handwerker, Experimental and Thermodynamic Assessment of Sn-Ag-Cu Solder Alloys, *J. Electron. Mater.*, 2000, **29**(10), p 1122–1136. https://doi.org/10.1007/s11664-000-0003-x
47. J. Miettinen, Thermodynamic Description of the Cu-Al-Sn System in the Copper-Rich Corner, *Metall. and Mater. Trans. A.*, 2002, **33**(6), p 1639–1648. https://doi.org/10.1007/s11661-002-0173-7
48. X.J. Liu, C.P. Wang, I. Ohnuma, R. Kainuma, and K. Ishida, Experimental Investigation and Thermodynamic Calculation of the Phase Equilibria in the Cu-Sn and Cu-Sn-Mn Systems, *Metallurgical and Mater. Trans. A*, 2004, **35**(6), p 1641–1654. https://doi.org/10.1007/s11669-018-0687-3
49. W. Gierlotka, S.W. Chen, and S.K. Lin, Thermodynamic Description of the Cu-Sn System, *J. Mater. Res.*, 2007, **22**(11), p 3158–3165. https://doi.org/10.1557/JMR.2007.0396
50. J. Miettinen, Thermodynamic Description of the Cu-Fe-Sn System at the Cu-Fe Side, *Calphad*, 2008, **32**(3), p 500–505. https://doi.org/10.1016/j.calphad.2008.06.003
51. M. Li, Z.M. Du, C.P. Guo, and C.R. Li, Thermodynamic Optimization of the Cu-Sn and Cu-Nb-Sn Systems, *J. Alloy. Compd.*, 2009, **477**(1–2), p 104–117. https://doi.org/10.1016/j.jallcom.2008.09.141
52. D. Li, P. Franke, S. Furtauer, D. Cupid, and H. Flandorfer, The Cu-Sn Phase Diagram part II: New Thermodynamic Assessment, *Intermetallics*, 2013, **34**, p 148–158. https://doi.org/10.1016/j.intermet.2012.10.010
53. H.Q. Dong, V. Vuorinen, X.M. Tao, T. Laurila, and M. Paulasto-Krockel, Thermodynamic Reassessment of Au-Cu-Sn Ternary System, *J. Alloy. Compd.*, 2014, **588**, p 449–460. https://doi.org/10.1016/j.jallcom.2013.11.041
54. B. Sundman, H.L. Lukas, and S.G. Fries, *Computational Thermodynamics: The Calphad Method*. Cambridge University Press, New York, 2007.
55. H. Flandorfer, U. Saeed, C. Luef, A. Sabbar, and H. Ipser, Interfaces in Lead-Free Solder Alloys: Enthalpy of Formation of Binary Ag–Sn, Cu–Sn and Ni–Sn Intermetallic Compounds, *Thermochim. Acta*, 2007, **459**(1–2), p 34–39. https://doi.org/10.1016/j.tca.2007.04.004
56. O.J. Kleppa, Heat of Formation of Solid and Liquid Binary Alloys of Copper with Cadmium, Indium, Tin and Antimony at 450°, *J. Phys. Chem.*, 1956, **60**(7), p 852–858. https://doi.org/10.1021/j150541a005
57. S. Ramos De Debiaggi, C. Deluque Toro, G.F. Cabeza, and A. Fernández Guillermet, Ab Initio Comparative Study of the Cu–In and Cu–Sn Intermetallic Phases in Cu–In–Sn Alloys, *J. Alloys and Compounds*, 2012, **542**, p 280–292. https://doi.org/10.1016/j.jallcom.2012.06.138
58. A. Jain, P.S. Ong, G. Hautier, W. Chen, W.D. Richards, S. Dacek, S. Cholia, D. Gunter, D. Skinner, G. Ceder, and K. Persson, Commentary: The Materials Project: A Materials Genome Approach to Accelerating Materials Innovation, *APL Mater.*, 2013, **1**, p 1011002. https://doi.org/10.1063/1.4812323